中国光学 Chinese Optics 核心期刊

复介质对光量子阱光传输特性的激活效应

苏安，蒙成举，江思婷，高英俊

引用本文:
苏安, 蒙成举, 江思婷, 高英俊. 复介质对光量子阱光传输特性的激活效应[J]. 中国光学, 2020, 13(2): 396-410. doi: 10.3788/CO.20201302.0396
SU An, MENG Cheng-ju, JIANG Si-ting, GAO Ying-jun. Activation effect of complex medium on the optical propagation properties of optical quantum well[J]. *Chinese Optics*, 2020, 13(2): 396-410. doi: 10.3788/CO.20201302.0396

在线阅读 View online: https://doi.org/10.3788/CO.20201302.0396

文章编号　2095-1531(2020)02-0396-15

Activation effect of complex medium on the optical propagation properties of optical quantum well

SU An[1], MENG Cheng-ju[1*], JIANG Si-ting[1], GAO Ying-jun[2]

(1. *Department of Physics and Electronic Engineering*, *Hechi University*, *Yizhou* 546300, *China*;
2. *College of Physical Science and Engineering*, *Guangxi University*, *Nanning* 530004, *China*)
* *Corresponding author*, *E-mail*: *mengchengju*@163. *com*

Abstract: By using the transmission matrix, the activation effect of complex medium on the optical propagation properties of optical quantum well has been studied. The result shows that, the light transmissivity and internal local electric field of an optical quantum well can be activated by complex medium. There is always an internal local electric field in the optical quantum well made of whether real medium or complex medium. The local electric field will always cause the frequency quantization and the appearance of discrete narrow transmission peaks in the transmission spectrum. Active impurities are added to the medium A. When the imaginary part of dielectric constant of complex medium, namely k, is positive, both the local electric field in the optical quantum well and the transmissivity of discrete narrow transmission peaks will be attenuated. With the increase of k value, the monotonic attenuation of internal local electric field becomes more obvious. However, the sensitivity of the response of local electric field to the positive imaginary part k is different at different wavelengths of optical quantum well, and the electric field at the central wavelength of the quantum well is the most sensitive to the k value. When the imaginary part of dielectric constant of complex medium, is negative, both the local electric field in the optical quantum well and the transmissivity of discrete narrow transmission peaks will have an amplified gain. As the value of negative imaginary part $|k|$ increases, the internal local electric field will increase to a maximal value and then become attenuated. However, the maximal value of the local electric field in gain amplification and the corresponding $|k|$ value are different at different wavelengths of the quantum well. To be specific, the local electric field in the short-wave direction of the quantum well is the most sensitive to $|k|$ value, while the local electric field in the long-wave direction is the least sensitive to $|k|$ value. The modulation mechanism of complex medium towards the light transmission characteristics of optical quantum well has positive guiding significance for the theoretical research and practical design of new optical filters, optical amplifiers and optical holophotes, and for the research of internal mechanism of light transmission characteristics of an optical quantum well.

Key words: complex-medium optical quantum well; activation; local electric field; transmission spectrum; optical device

收稿日期:2019-05-06;**修订日期**:2019-7-11

基金项目:国家自然科学基金(No. 51161003);河池学院 2018 年高层次人才科研启动费项目(No. XJ2018GKQ017);广西高校中青年教师基础能力提升项目(No. 2018 KY 0501);国家级大学生创新计划训练项目(No. 201910605016)

Supported by National Natural Science Foundation of China(No. 51161003); Hechi University's 2018 High-level Talents Scientific Research Start-up Project (No. XJ2018GKQ017); Guangxi Colleges and Universities' Young and Middle-aged Teachers' Basic Ability Improvement Project (No. 2018ky0501) and National College Students' Innovation Plan Training Project (No. 201910605016)

复介质对光量子阱光传输特性的激活效应

苏 安[1],蒙成举[1*],江思婷[1],高英俊[2]
(1. 河池学院 物理与机电工程学院,宜州 546300;
2. 广西大学 物理科学与工程技术学院,南宁 530004)

摘要: 利用传输矩阵法研究复介质对光量子阱光传输特性的激活效应机制,结果表明复介质可有效激活光量子阱的光透射率和内部局域电场。无论组成光量子阱的介质是实介质还是复介质,光量子阱内部均存在局域电场,且局域电场均会产生频率量子化并在透射谱中出现分立的窄透射峰。在介质 A 中掺入激活性杂质的复介电常数虚部 k 为正时,光量子阱内部局域电场和分立窄透射峰的透射率均出现衰减现象,且随着 k 值增大内部局域电场单调衰减越来越明显,但光量子阱不同波长位置的局域电场对 k 值的响应灵敏度不同,其中光量子阱中心波长处对应的电场对 k 值响应最灵敏;当复介电常数的虚部 k 为负值时,光量子阱内部局域电场和分立窄透射峰的透射率均出现增益放大现象,随着负虚部 $|k|$ 值增大,内部局域电场先增大至极大值随后衰减,但光量子阱不同波长位置的局域电场增益放大的极大值及其对应的 $|k|$ 值大小不同,其中光量子阱短波方向局域电场对 $|k|$ 值响应最灵敏,长波方向局域电场对 $|k|$ 值响应灵敏度最低。研究复介质对光量子阱光传输特性的调制机制,对新型光学滤波器、光学放大器和光学全反射镜的理论研究与实际设计,以及光量子阱光传输特性的内在机制研究等,均具有积极的指导意义。

关 键 词: 复介质光量子阱;激活;局域电场;透射谱;光学器件
中图分类号: O431;O483;O734 **文献标识码:** A doi:10.3788/CO.20201302.0396

1 Introduction

It is well known that semiconductor materials and their technology have revolutionized the technology of information transmission. However, with the increasing demand and the limitation of production design and process, the information transmission speed and process integration of semiconductor communication devices have almost reached their limits, that is, the information technology with electronics as the information transmission carrier has encountered a "bottleneck" in its development. So the researchers begin to shift their focus on photons, which have irreplaceable advantages over electrons, such as extremely fast propagation speed, large transmission capacity and no interaction. Therefore, photons has been expected to replace electrons for information transmission since the birth of photonic crystal concept[1-2]. The use of photonic crystal as the carrier of information transmission will also spark a new round of information technology revolution. Photonic crystal is a kind of artificial micro-structured optical material formed by the thin films in ordered arrangement and with different permittivities. Its strangest and most attractive characteristic is that it can be selectively passed by some light frequencies. Moreover, its transmission behavior can be manually controlled by reasonable structure adjusting or impurity adding. This characteristic is of great practical significance for efficient information transmission by light[3-8].

A large number of research results show that when a periodic photonic crystal is defective or doped with impurities, the propagation of light to the defects will cause the appearance of local photonic state, in which a strong local electric field will exist. Because light is confined to the local state, the photonic state density in that area will be very high and finally the transmission peaks (defect mode) with high transmittance and narrow bandwidth will be formed at the macro level[9-13]. It can be seen that the effect of strong local electric field in the photonic crystal can be used to realize optical filtering very well. Therefore, how to reasonably design and produce local photonic states in photonic crystals and how to enhance the density of local photonic states are not only the problems to be solved, but also the focuses of research. As a result, the researchers have designed a photonic crystals quantum well (PQW) structure with stronger internal effects on optical localization. The optical quantum well structure is composed of a well layer and a barrier layer. Due to the restriction of the barrier layer on both sides, light is highly localized in the quantum well. This highly localized electric field will result in the frequency quantization. The quantized light will pass through the photonic crystal through resonance tunneling and form discrete transmission peaks with ultra-narrow bandwidth, thus providing theoretical support for the realization of high-quality optical filtering[13-18].

In recent years, the researchers have further added active impurities (such as erbium, etc.) to the PQW medium to obtain better optical filtering effect. The results show that the active impurities have a good modulation effect on the light transmission characteristics of optical quantum well. Especially, they have an amplification effect on the light transmission of the quantum well, which is generated by the frequency quantization of local electric field in the well[4,11,14,19-20]. Therefore, there must be some correlation between the amplification effect on transmission characteristics and the internal local electric field, that is, the problem is whether the internal mechanism of this light amplification effect is the amplification of internal local electric field by active impurities. Based on this thinking, this research project has especially studied the gain amplification mechanism of active impurities on the local electric field in an optical quantum well by establishing the PQW structure model and adding active impurities to the medium. The research results will provide theoretical guidance for the design of optical amplifiers and filters in the optical quantum well.

2 Research method and PQW structure model

2.1 Research method

The main objects of this project are the transmittance and internal local electric field of an optical quantum well, so the transmission matrix method is used for their calculation and exploration. The core of transfer matrix method is to convert the Maxwell equation of light transmission in thin film medium into a transmission matrix. Then the total transmission behavior of light in the whole periodic film medium (photonic crystal) is equal to the product of the transmission sub-matrices of light in all the medium layers, so the process of solving the Maxwell equation of electromagnetic field transmission in a photonic crystal can be converted into the process of solving the eigenvalue problem. The transmission matrix method is a visualized method with few matrix elements and high computational efficiency. It is especially advantageous in the calculation of transmittance, reflectance, electric field distribution, and dispersion curve[4-5, 13-18]. As the transmission matrix has been widely used, it will not be repeated here.

2.2 PQW structure model

The constructed PQW structure model is $(AB)^m(ABA)^n(BA)^m$, as illustrated in Fig. 1. In the model, $(AB)^m(BA)^m$ is the barrier layer of optical quantum well, and $(ABA)^n$ is the well layer of optical quantum well. m and n are respectively the number of permutation cycles in the barrier layer and well layer of a photonic crystal, and can be rounded into positive integers in calculation, research and actual design. Judging from model structure, the optical quantum well $(AB)^m(ABA)^n(BA)^m$ is a structure of mirror symmetry. In the model, A and B are thin film medium and their material, permittivity and physical thickness are as follows: A: AsS, $\varepsilon_A = 6.760$, $d_A = 741.0$ nm; B: SiO_2, $\varepsilon_B = 2.1025$, $d_B = 1\ 329.0$ nm. If active impurities are added to the medium, the permittivity of the medium will be a complex number and the medium will also be called complex medium. When the imaginary part of complex permittivity is positive, light will be attenuated; when the imaginary part of permittivity is negative, light will be gained and amplified[4,11,14,19-20]. The energy band structures of the photonic crystals $(AB)^5(BA)^5$ and $(ABA)^{10}$ can be drawn through Matlab (a scientific computing software) programming, as shown in Fig. 2.

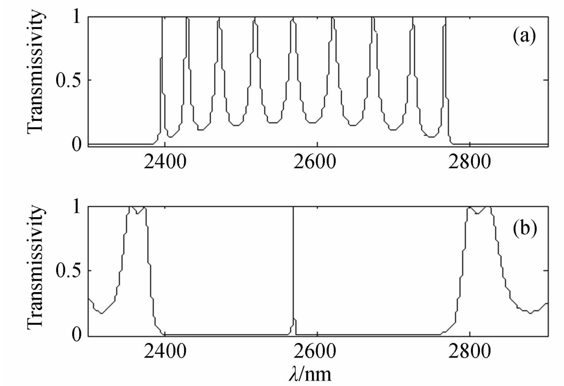

Fig. 2　Band-gap structure of 1D photonic crystals. (a) $(ABA)^{10}$; (b) $(AB)^5(BA)^5$

图 2　一维光子晶体的带隙结构。(a) $(ABA)^{10}$; (b) $(AB)^5(BA)^5$

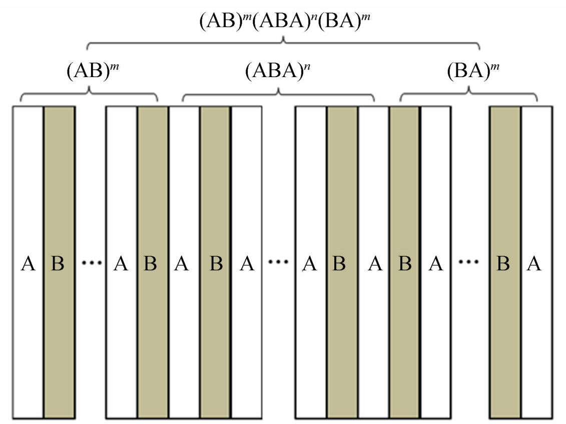

Fig. 1　Structural diagram of 1D photonic crystal well

图 1　一维光子晶体量子阱结构示意图

As can be seen from Fig. 2, in the wavelength range of 2 381 ~ 2 789 nm, the passband of the well-layer photonic crystal $(ABA)^{10}$ falls completely into the forbidden band of the barrier-layer photonic crystal $(AB)^5(BA)^5$, that is, the photonic crystal $(AB)^m(ABA)^n(BA)^m$ reasonably constitutes a PQW structure. When the medium is doped with active impurities to form the complex medium, the optical quantum well is a quantum well structure containing complex medium, complex-medium optical quantum well for short.

3　Calculation results and analysis

3.1　Transmission spectrum and internal electric field distribution of quantum well in real medium

First, with other parameters unchanged, define the number of barrier-layer cycles of the optical quantum well $(AB)^m(ABA)^n(BA)^m$ as $m = 3$ and the number of well-layer cycles as $n = 2$, 3 and 4 in progressive increase. Considering the vertical incidence of light, the transmission spectrum of the optical quantum well $(AB)^3(ABA)^n(BA)^3$ can be drawn through Matlab programming and simulation, as shown in Fig. 3. In the figure, the abscissa is the wavelength of incident light, and the ordinate is the transmittance.

As can be seen from Fig. 3, when the thin film media composing of the optical quantum well are all real media, a wide forbidden band will appear in the wavelength range of 2 381-2 789 nm. There are discrete narrow transmission peaks with 100% transmittance in the forbidden band. The number of transmission peaks is related to the number of permutation cycles (n) of the well-layer photonic crystal $(ABA)^n$ and is equal to $n - 1$. In addition, as can be seen from Fig. 3, with the increase of the num-

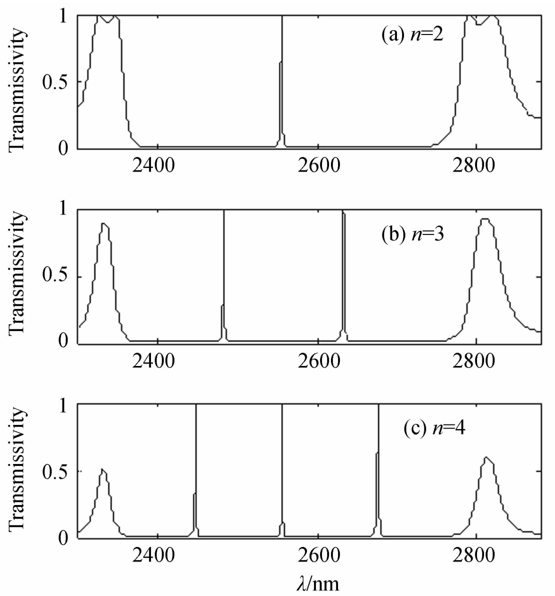

Fig. 3 Transmission spectra of PQW$(AB)^3(ABA)^n(BA)^3$

图 3 光量子阱$(AB)^3(ABA)^n(BA)^3$的透射谱

ber of permutation cycles (n), the number of discrete narrow transmission peaks will increase, while the bandwidth of transmission peaks and the distance between transmission peaks will decrease. The comparison between Fig. 3 and Fig. 2 shows that, the wavelength range in the transmission spectrum shown in Fig. 3, where discrete narrow transmission peaks appear, is exactly the wavelength range in Fig. 2 where the quantum well structure is formed. Therefore, when light is transmitted to the optical quantum well, the localization effect of quantum well structure on the light will limit the light propagation. This strong localization effect results in the frequency quantization of light field in the quantum well. The quantized light passes through the quantum well in the way of resonance tunneling, forming discrete narrow transmission peaks in the transmission spectrum. Moreover, as the number of well-layer cycles increases, the range of frequency quantization will be enlarged and the quantization degree will be intensified, that is, the wavelength range of discrete transmission peaks will increase and their bandwidth will decrease. This light-transmission characteristic of optical quantum well has important guiding significance for the design and manufacture of optical filters with high performance.

Then, the local electric field distribution inside the quantum well can be plotted. Given the number of well-layer cycles ($n=4$), the corresponding wavelengths of three discrete narrow transmission peaks, namely $\lambda_1=2\ 447.72$ nm, $\lambda_2=2\ 556.21$ nm and $\lambda_3=2\ 675.13$ nm, are taken as the incident wavelengths for calculating the internal local electric field. The local electric field distribution in the optical quantum well $(AB)^3(ABA)^4(BA)^3$ is shown in Fig. 4(b-d). In the figure, the abscissa z is the propagation position of light in the optical quantum well, and the ordinate $|E/E_0|$ is the relative value of the local electric field. The Fig. 4(a) shows the transmission spectrum of the quantum well $(AB)^3(ABA)^4(BA)^3$.

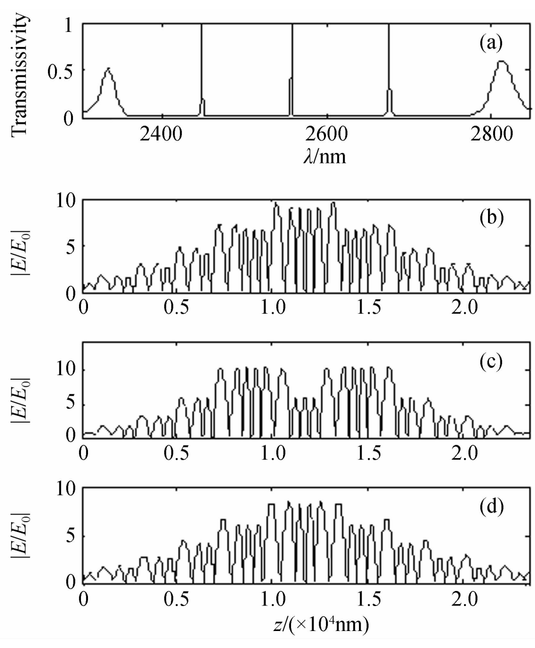

Fig. 4 Transmission spectrum and electric field distributions of PQW$(AB)^3(ABA)^4(BA)^3$

图 4 $(AB)^3(ABA)^4(BA)^3$的透射谱与电场分布

As can be seen from Fig. 4, when light propagates into the structure of optical quantum well, a strong local electric field is formed inside the quantum well. When the wavelength of incident light is $\lambda_1 = 2\ 447.72$ nm, the maximum value of local electric field inside the quantum well is $|E/E_0|_{max} = 9.531$; when the wavelength of incident light is $\lambda_2 = 2\ 556.21$ nm, the maximum value of internal local electric field is $|E/E_0|_{max} = 10.29$; when the wavelength of incident light is $\lambda_3 = 2\ 675.13$ nm, the maximum value of internal local electric field is $|E/E_0|_{max} = 8.394$, as shown in Fig. 4(b-d). It can also be seen from Fig. 4 (a) that, the narrow transmission peak $\lambda_2 = 2\ 556.21$ nm is located at the center of the quantum well, and has a narrower bandwidth than the discrete transmission peaks on both sides. When being calculated based on this wavelength, the local electric field inside the quantum well will be the maximum. This indicates that the light field incident to the quantum well structure is localized in the quantum well. The closer it is to the center of the well, the more localized it is.

3.2 Transmission spectrum and internal electric field distribution of quantum well in complex medium

We still take the optical quantum well structure $(AB)^3(ABA)^4(BA)^3$ as the research object. Suppose that other parameters remain unchanged, and add active impurities to the medium A. First, consider the doping with the active impurities with attenuation effect. Then the permittivity of the medium will be a complex number with positive imaginary part[19-20]. In this case, the optical quantum well structure is called complex-medium optical quantum well structure. Suppose $\varepsilon_A = 6.670 + 0.1i$. The transmission spectrum and internal electric field distribution of the complex-medium optical quantum well $(AB)^3(ABA)^4(BA)^3$ can be drawn, as shown in Fig. 5 (a-d).

Firstly, as can be seen from Fig. 5, when the medium A of the quantum well is doped with the impurities with attenuation effect, the light transmission and internal local electric field of the quantum well will show different degrees of attenuation. The comparison between Fig. 5 and Fig. 4 shows that, when the medium A is a complex medium with attenuation effect, three narrow transmission peaks of the optical quantum well $(AB)^3(ABA)^4(BA)^3$ will appear at $\lambda_1 = 2\ 447.72$ nm, $\lambda_2 = 2\ 556.21$ nm and $\lambda_3 = 2\ 675.13$ nm respectively. Their transmittances will decrease from 100% in the real medium to 23.43%, 17.29% and 21.25% respectively. When taking $\lambda_1 = 2\ 447.72$ nm, $\lambda_2 = 2\ 556.21$ nm and $\lambda_3 = 2\ 675.13$ nm as incident wavelengths to calculate the internal local electric field, the maximum values of internal local electric field will be attenuated from $|E/E_0|_{max} = 9.531$, 10.29 and 8.394 in real medium to $|E/E_0|_{max} = 4.736$, 4.376 and 3.965 in complex medium. Therefore, the internal cause of the transmittance attenuation of discrete narrow transmission peaks in the transmission spectrum is that active impurities with attenuation effect is added into medium of optical quantum well, which results in attenuation of internal local electric field.

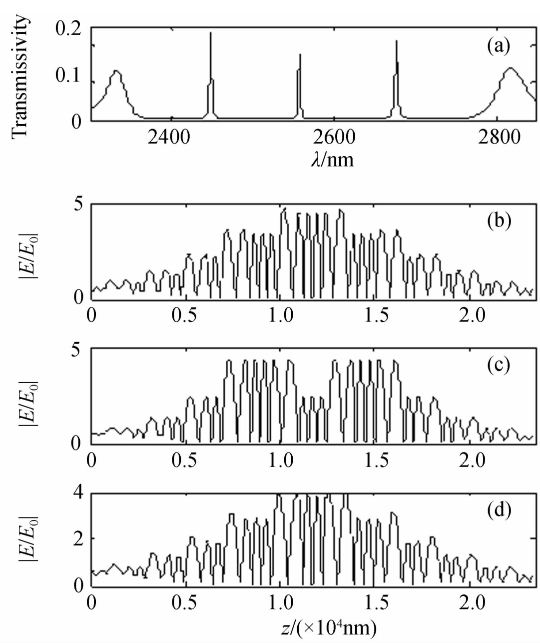

Fig. 5　Transmission spectrum and electric field distributions of PQW$(AB)^3(ABA)^4(BA)^3$ with ε_A of $6.670 + 0.1i$

图 5　$\varepsilon_A = 6.670 + 0.1i$ 时$(AB)^3(ABA)^4(BA)^3$的透射谱与电场分布

Secondly, when the medium A is doped with the activated impurities with gain effect, the permittivity of the medium is a complex number with negative imaginary part[19-20]. Suppose $\varepsilon_A = 6.670 - 0.02i$. The transmission spectrum and internal local electric field distribution of the complex-medium optical quantum well $(AB)^3(ABA)^4(BA)^3$ can be drawn, as shown in Fig. 6 (a-d).

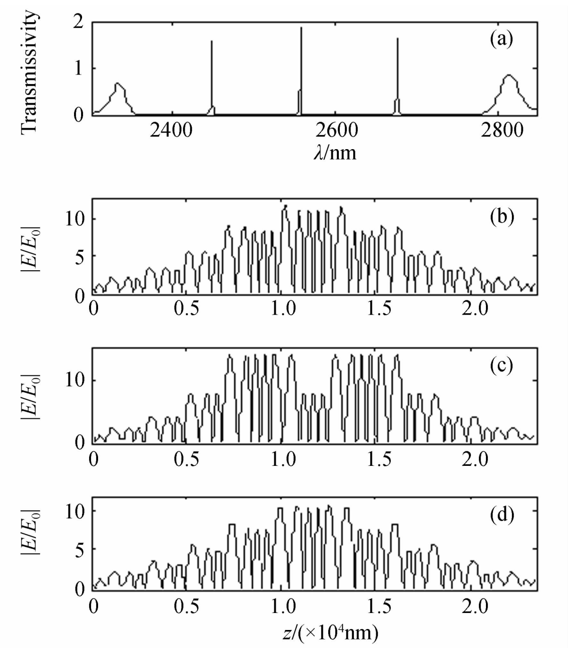

Fig. 6 Transmission spectrum and electric field distributions of PQW$(AB)^3(ABA)^4(BA)^3$ with ε_A of $6.670-0.02i$

图6 $\varepsilon_A = 6.670-0.02i$ 时$(AB)^3(ABA)^4(BA)^3$的透射谱与电场分布

As can be seen from Fig. 6, when the medium A of the optical quantum well is doped with the active impurities with gain effect, the discrete narrow transmission peaks and internal local electric field of the quantum well will show gain amplification of different degrees. The comparison between Fig. 6 and Fig. 4 shows that, when the medium A is a complex medium with gain effect, three narrow transmission peaks of the optical quantum well $(AB)^3(ABA)^4(BA)^3$ will appear at $\lambda_1 = 2\ 447.72$ nm, $\lambda_2 = 2\ 556.21$ nm and $\lambda_3 = 2\ 675.13$ nm respectively. Their transmittances will increase through gain amplification from 100% in the real medium to 156.85%, 186.45% and 164.96% respectively. When taking $\lambda_1 = 2\ 447.72$ nm, $\lambda_2 = 2\ 556.21$ nm and $\lambda_3 = 2\ 675.13$ nm as incident wavelengths to calculate the internal local electric field, the maximum values of internal local electric field will be increased through gain from $|E/E_0|_{max} = 9.531$, 10.29 and 8.394 in real medium to $|E/E_0|_{max} = 11.85$, 14.00 and 10.69 in complex medium. Thus it can be seen that the addition of the active impurities with gain effect to the medium A will amplify the gain of the local electric field inside the quantum well, and the gain of the transmittance of discrete transmission peaks in the transmission spectrum.

3.3 Response of internal local electric field to the imaginary part of complex medium

We still take the optical quantum well structure $(AB)^3(ABA)^4(BA)^3$ as the research object. Taking the imaginary part k of complex medium as abscissa and the maximum value of the local electric field $|E/E_0|$ as the ordinate, the response of local electric field to active impurities can be plotted. When the medium A is doped with the active impurities with attenuation effect, namely $\varepsilon_A = 6.670 + ki$, the response curves $|E/E_0| \sim k$ of the maximum values of internal local electric field to active impurities can be calculated by assigning $k = 0, 0.04, 0.06..., 0.12, 0.16$ and $\lambda_1 = 2\ 447.72$ nm、$\lambda_2 = 2\ 556.21$ nm, $\lambda_3 = 2\ 675.13$ nm (incident wavelengths), as shown in Fig. 7.

As can be seen from Fig. 7, when the medium A is doped with the active impurities with attenuation effect or when the permittivity of the medium A is a complex number containing the positive imaginary part k, the maximum value of the local electric field $|E/E_0|$ inside the quantum well will be attenuated with the increase of k. Moreover, the attenuation speed of the maximum value of internal local electric field varies with incident wavelength. When the wavelength $\lambda_2 = 2\ 556.21$ nm corresponding to the central transmission peak of the quantum well is taken as incident wavelength, the maximum value of the internal local electric field $|E/E_0|$ has the fastest attenuation rate. When the wavelength $\lambda_1 =$ 2 447.72 nm corresponding to the transmission peak in the short-wave direction is taken as incident wavelength, the maximum value of the internal local electric field $|E/E_0|$ has the second-fastest attenuation rate. When the wavelength $\lambda_3 = 2\ 675.13$ nm corresponding to the transmission peak in the long-wave direction is taken as incident wavelength, the maximum value of the internal local electric field $|E/E_0|$ has the slowest attenuation rate. It can be further inferred that when the positive imaginary part k increases to a certain value, the local electric field inside the quantum well will approach zero. At this point, the transmittance of discrete transmission peaks is zero at the macro level, that is, the optical quantum well can achieve the function of optical holophote.

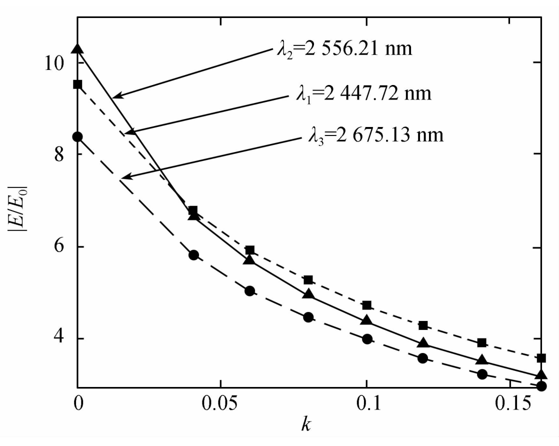

Fig. 7 Electric field distributions versus k of PQW $(AB)^3(ABA)^4(BA)^3$ with ε_A of $6.670 + k\mathrm{i}$

图 7 $\varepsilon_A = 6.670 + k\mathrm{i}$ 时, k 对 $(AB)^3(ABA)^4(BA)^3$ 内部电场的影响

When the medium A is doped with the active impurities with gain effect, namely $\varepsilon_A = 6.670 - k\mathrm{i}$, the response curves $|E/E_0| \sim k$ of the maximum values of internal local electric field to active impurities can be calculated by assigning $k = 0$, 0.04, 0.06..., 0.12, 0.16 and $\lambda_1 = 2\ 447.72$ nm, $\lambda_2 = 2\ 556.21$ nm, $\lambda_3 = 2\ 675.13$ nm (incident wavelengths), as shown in Fig. 8.

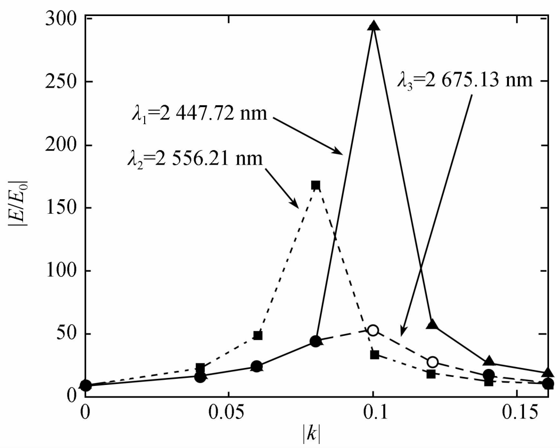

Fig. 8 Electric field distributions versus k of PQW $(AB)^3(ABA)^4(BA)^3$ with ε_A of $6.670 - k\mathrm{i}$

图 8 $\varepsilon_A = 6.670 - k\mathrm{i}$ 时, k 对 $(AB)^3(ABA)^4(BA)^3$ 内部电场的影响

As can be seen from Fig. 8, when the medium A is doped with the active impurities with gain effect or when the permittivity of the medium A is a complex number containing the negative imaginary part, with the increase of $|k|$, the maximum value of the local electric field $|E/E_0|$ inside the quantum well will increase, reach an extreme value, and then decrease. Moreover, at different incident wavelengths, the maximum value of the internal local electric field $|E/E_0|$ will have different inflection points towards the extreme value. When the wavelength $\lambda_1 =$ 2 447.72 nm corresponding to the transmission peak in the short-wave direction is taken as incident wavelength, the infection point will appear at the maximum value of internal local electric field $|E/E_0| =$ 299.60 given that $|k| = 0.10$. When the wavelength $\lambda_2 = 2\ 556.21$ nm corresponding to the central transmission peak is taken as incident wavelength, the infection point will appear at the maximum value of internal local electric field $|E/E_0| = 166.50$ given that $|k| = 0.08$. When the wavelength $\lambda_3 =$ 2 675.13 nm corresponding to the transmission peak in the long-wave direction is taken as incident wavelength, the infection point will appear at the maximum value of internal local electric field $|E/E_0|=52.196$ given that $|k|=0.10$. It can be seen that when the medium A is doped with the active impurities with gain effect, gain amplification will occur to the local electric field inside the quantum well in the same trend, namely increasing first and then attenuation. However, the extreme values of internal local electric field under gain amplification and the corresponding negative imaginary part are different at different wavelengths.

4 Conclusion

Through the transmission matrix method, the response of light transmission characteristics in the optical quantum well to complex medium has been studied to achieve the following conclusions:

(1) Whether made of real medium or complex medium, local electric field in optical quantum well will always cause the frequency quantization and the appearance of discrete narrow transmission peaks in the transmission spectrum;

(2) When the imaginary part of permittivity of the complex medium doped with active impurities, namely k, is positive, both the local electric field in the optical quantum well and the transmittance of discrete narrow transmission peaks will be attenuated. With the increase of k value, the monotonic attenuation of internal local electric field becomes more obvious. However, the sensitivity of the response of local electric field to the positive imaginary part k is different at different wavelengths of optical quantum well, and the local electric field at the central wavelength of the quantum well is the most sensitive to the k value;

(3) When the imaginary part of permittivity of the complex medium doped with active impurities, namely k, is negative, both the local electric field in the optical quantum well and the transmittance of discrete narrow transmission peaks will have an amplified gain. As the value of negative imaginary part $|k|$ increases, the internal local electric field will increase to a maximal value and then become attenuated. However, the maximal value of the local electric field at different wavelengths in gain amplification and is corresponding to different $|k|$ value. To be specific, the local electric field in the short-wave direction is the most sensitive to $|k|$ value, while the local electric field in the long-wave direction is the least sensitive to $|k|$ value.

The modulation mechanism of complex medium to the light transmission characteristics of optical quantum well has a positive reference value for the research and design of the functions of new optical filters, optical amplifiers and optical holophotes.

——中文对照版——

1 引 言

众所周知,半导体材料及相关技术给信息传输技术带来了革命性的影响。但随着实际需求的提升和生产设计、工艺的限制,半导体通信器件的信息传输速度和工艺集成度已接近极限,即以电子为信息传输载体的信息技术发展遇到“瓶颈”。于是,研究者把目光聚焦到光子,相比电子,光子具有传播速度极快、传输容量大、无相互作用等不可替代的优势。因此,从光子晶体[1-2]概念一诞生,光子就被寄予代替电子进行信息传输的厚望,而且以光子晶体作为信息传输载体也必将掀起新一轮的信息技术革命。光子晶体是一种由不同介电常数的薄膜介质有序排列形成的人工微结构光学材料,它最奇特也是最具有吸引力的特性是对光频率具有选择性通过,并且通过合理的结构调整或掺杂杂质可人为控制光的传输行为。这种特性对利用光实现高效率的信息传输具有极其重要的实际意义[3-8]。

大量的研究结果表明,当周期性排列的光子晶体内存在缺陷或是介质中掺入杂质时,光传播到缺陷或杂质处会出现局域光子态,局域光子态中存在很强的局域电场,由于光被限制在局域态里致使该处的光子态密度很高,最终导致在宏观上形成透射率很高且带宽很窄的透射峰(缺陷模)[9-13]。可见,利用光子晶体内部强局域电场产生的效应可很好地实现光学滤波功能。因此,怎样通过合理设计以在光子晶体内部产生局域光子态以及如何增强局域光子态密度等,既是要解决的问题也是研究的重点。于是,研究者们又设计出内部对光局域作用更强的光子晶体量子阱结构,简称光量子阱(Photonic crystals Quantum Well, PQW)。光量子阱结构由阱层和垒层组成,由于两侧垒层的限制作用,使光被高度局域在量子阱内,这种被高度局域的电场将产生频率量子化,量子化后的光通过共振隧穿的方式透射光子晶体并形成超窄带的分立透射峰,为实现高品质的光学滤波功能提供了理论支撑[13-18]。近年来,研究者们还进一步地在光子晶体量子阱的介质中掺入激活性杂质(如铒等),以获得更高性能的光学滤波效果。研究成果显示,激活性杂质对光量子阱的光传输特性具有很好的调制作用,尤其是对光量子阱的光透射具有放大效应,而光量子阱的透射特性是由阱内局域电场的频率量子化产生的[4,11,14,19-20]。因此,透射特性的光放大效应与内部局域电场也必然存在某种关联性,即透射特性光放大效应的内在机制是否是由于激活性杂质对内部局域电场的放大导致的?基于这种思考,本课题组在构造光子晶体量子结构模型的基础上,在介质中掺入激活性杂质,重点研究激活性杂质对光量子内部局域电场的增益放大机制等,本文研究结果为利用光量子阱结构设计光学放大器、光学滤波器等提供理论指导。

2　研究方法与光量子阱结构模型

2.1　研究方法

本课题计算和研究的主要对象为光量子阱的透射率和内部局域电场,所以研究方法采用传输矩阵法。传输矩阵法的原理是把光在薄膜介质中传输的麦克斯韦方程转化成传输矩阵形式,则光在周期性排列的薄膜介质整体(光子晶体)中的总传输行为等于在各分层介质中的分矩阵之积,从而把电磁场在光子晶体中传播的麦克斯韦方程转化为求解本征值问题。传输矩阵法形象直观,且矩阵元少,计算效率高,尤其在计算透射率、反射率、电场分布和色散曲线等方面具有优势[4-5,13-18]。传输矩阵的使用已经很广泛,在此不再赘述。

2.2　光量子阱结构模型

本文构造的光子晶体量子阱结构模型为$(AB)^m(ABA)^n(BA)^m$,如图1所示。其中$(AB)^m$ $(BA)^m$是光量子阱的垒层,$(ABA)^n$是光量子阱的阱层,m 和 n 分别是垒层、阱层光子晶体的排列周期数,在计算、研究和实际设计时可取正整数。从模型结构看,$(AB)^m(ABA)^n(BA)^m$光量子阱为镜像对称结构。模型中的A、B为薄膜介质,它们对应的物质、介电常数及物理厚度分别如下:A为硫化砷(AsS),$\varepsilon_A=6.760$,$d_A=741.0$ nm;B为二氧化硅(SiO_2),$\varepsilon_B=2.1025$,$d_B=1329.0$ nm。若在介质中掺入激活性杂质,则介质的介电常数为复数,介质亦称为复介质,复介质的介电常数的虚部为正时对光具有衰减效应,复介质的介电常数的虚部为负值时对光具有增益放大效应[4,11,14,19-20]。通过科学计算软件Matlab编程计算,可绘制出光子晶体$(AB)^5(BA)^5$和$(ABA)^{10}$的能带结构,如图2所示。

由图2可见,在2381~2789 nm波长范围内,阱层光子晶体$(ABA)^{10}$的通带完全处于垒层光子晶体$(AB)^5(BA)^5$的禁带中,即光子晶体$(AB)^m(ABA)^n(BA)^m$很合理地构成了光子晶体量子阱结构。当介质中掺入激活性杂质形成复介质时,光量子阱为含有复介质的光量子阱结构,简称复介质光量子阱。

3　计算结果与分析

3.1　实介质光量子阱的透射谱及内部电场分布

首先在其他参数不变的情况下,固定光量子

阱$(AB)^m(ABA)^n(BA)^m$的垒层周期数$m=3$,取阱层周期数n分别为2、3、4,依次递增。考虑光垂直入射的情形,通过科学计算软件Matlab编程计算仿真,可绘制出光量子阱$(AB)^3(ABA)^n(BA)^3$的透射谱,如图3所示,图中横坐标为入射光的波长,纵坐标为透射率。

由图3可知,当组成光量子阱的薄膜介质全是实介质时,在2 381~2 789 nm波长范围内出现了一条很宽的禁带,在禁带中出现了透射率为100%的分立窄透射峰,而且透射峰的数目与阱层光子晶体$(ABA)^n$排列周期数n相关,并等于$n-1$。另外,从图3还可以看到,随着排列周期数n的增大,分立窄透射峰数目增加的同时,透射峰的带宽越来越窄,而且透射峰之间的距离也越来越小。比较图3和图2可知,图3透射谱中分立窄透射峰出现的波长范围恰好是图2光量子阱结构形成的波长范围。由此说明,当光传输到光量子阱中时,由于光量子阱结构对光的局域作用限制了光的传播,这种强局域作用导致光场在量子阱内发生频率量子化,量子化后的光以共振隧穿的方式通过光量子阱,形成透射谱中分立的窄透射峰。而且当阱层周期数越大时,频率量子化范围的扩大程度及量子化程度越高,即出现分立透射峰的波长范围越广以及透射峰的带宽越窄。光量子阱的这种光传输特性对设计制造高性能的光学滤波器件具有重要的指导意义。

进一步地,可绘制出光量子阱内部的局域电场分布,分别以光量子阱阱层周期数$n=4$时3条分立窄透射峰对应的波长,$\lambda_1=2\ 447.72$ nm、$\lambda_2=2\ 556.21$ nm和$\lambda_3=2\ 675.13$ nm,作为计算内部局域电场的入射波长,可得光量子阱$(AB)^3(ABA)^4(BA)^3$的内部局域电场分布如图4(b)~(d)所示,图中横坐标z为光在光量子阱中传播的位置,纵坐标$|E/E_0|$为局域电场相对值。图4(a)是光量子阱$(AB)^3(ABA)^4(BA)^3$的透射谱。

从图4可见,当光传播到光量子阱结构中时,光量子阱内部形成了很强的局域电场:入射光波长为$\lambda_1=2\ 447.72$ nm时,光量子阱内部局域电场最大值$|E/E_0|_{max}=9.531$;入射光波长为$\lambda_2=2\ 556.21$ nm时,内部局域电场最大值$|E/E_0|_{max}=10.29$;入射光波长为$\lambda_3=2\ 675.13$ nm时,内部局域电场最大值$|E/E_0|_{max}=8.394$如图4(b)~(d)所示。同时,从图4(a)可知,$\lambda_2=2\ 556.21$ nm的窄透射峰处于光量子阱的中心位置,且此透射峰比两侧的分立透射峰的带宽更窄,而以此波长计算得到的光量子阱内部局域电场值最大,说明当光入射到光量子阱结构时,光场被局域限制在量子阱里,而且越靠近阱中心,光被限制的程度越大。

3.2 复介质光量子阱透射谱及内部电场分布

仍然以光量子阱结构$(AB)^3(ABA)^4(BA)^3$为研究对象,其他参数固定不变,在介质A中掺入激活性杂质,首先考虑掺入具有衰减效应的激活性杂质,则介质介电常数为带正虚部的复数[19-20],此时光量子阱结构称为复介质光量子阱结构。假设$\varepsilon_A=6.670+0.1i$,可绘制出复介质光量子阱$(AB)^3(ABA)^4(BA)^3$的透射谱和内部电场分布,如图5所示。

从图5可见,当光量子阱的A介质中掺入衰减效应的杂质时,光量子阱的光透射及内部局域电场均出现不同程度的衰减现象。对比图5和图4可知:当介质A为衰减效应的复介质时,光量子阱$(AB)^3(ABA)^4(BA)^3$在$\lambda_1=2\ 447.72$ nm、$\lambda_2=2\ 556.21$ nm和$\lambda_3=2\ 675.13$ nm波长位置同样出现了3条窄透射峰,但透射率由实介质时的100%,分别衰减到23.43%、17.29%和21.25%。以$\lambda_1=2\ 447.72$ nm、$\lambda_2=2\ 556.21$ nm和$\lambda_3=2\ 675.13$ nm为入射波长计算内部局域电场时,内部局域电场的最大值$|E/E_0|_{max}$则由实介质时的9.531、10.29、8.394分别衰减到复介质时的4.736、4.376、3.965。可见,透射谱中分立窄透射峰透射率衰减的内因是由于组成光量子阱的介质中掺入了衰减效应的激活杂质,导致光量子阱内部局域电场的衰减。

其次,当介质A中掺入具有增益效应的激活

性杂质,且其介质介电常数为带负虚部的复数时[19-20],假设 $\varepsilon_A = 6.670 - 0.02i$,可绘制出复介质光量子阱$(AB)^3(ABA)^4(BA)^3$的透射谱和内部局域电场分布,如图 6 所示。

从图 6 可见,当光量子阱的 A 介质中掺入具有增益效应的激活性杂质时,光量子阱的分立窄透射峰及内部局域电场均出现了不同程度的增益放大现象。对比图 6 和图 4 可知:当介质 A 为增益效应的复介质时,光量子阱$(AB)^3(ABA)^4(BA)^3$在 $\lambda_1 = 2\ 447.72$ nm、$\lambda_2 = 2\ 556.21$ nm 和 $\lambda_3 = 2\ 675.13$ nm 3 个波长位置出现的窄透射峰,透射率由实介质时的 100%,分别增益放大到复介质时的 156.85%、186.45% 和 164.96%。以 $\lambda_1 = 2\ 447.72$ nm、$\lambda_2 = 2\ 556.21$ nm 和 $\lambda_3 = 2\ 675.13$ nm为入射波长计算内部局域电场,则内部局域电场的最大值 $|E/E_0|_{max}$ 由实介质时的 9.531、10.29、8.394 增益到复介质时的 11.85、14.00、10.69。由此可见,介质 A 中掺入增益效应的激活杂质可使光量子阱内部局域电场的增益放大,并导致透射谱中分立透射峰透射率的增益放大。

3.3　内部局域电场对复介电介质虚部的响应

仍然以光量子阱$(AB)^3(ABA)^4(BA)^3$为研究对象,以复介质的虚部 k 为横坐标,光量子阱内部局域电场的最大值$|E/E_0|$为纵坐标,可绘制出光量子阱内部局域电场对激活性杂质的响应情况。当 A 介质掺入衰减效应的激活杂质,即 $\varepsilon_A = 6.670 + k$i 时,取 $k = 0$、0.04、0.06...、0.12、0.16,分别以 $\lambda_1 = 2\ 447.72$ nm、$\lambda_2 = 2\ 556.21$ nm 和 $\lambda_3 = 2\ 675.13$ nm 为入射波长,计算出的内部局域电场最大值对激活性杂质的响应曲线$|E/E_0| \sim k$,如图 7 所示。

从图 7 可见,当 A 介质中掺入衰减效应的激活性杂质,即 A 介质的介电常数为含正虚部的复数时,光量子阱内部局域电场$|E/E_0|$最大值随正虚部 k 的增大而衰减,而且入射波长不同,内部局域电场最大值衰减的速度不一样,以光量子阱中心透射峰对应的波长 $\lambda_2 = 2\ 556.21$ nm 作为入射波长时,内部局域电场最大值$|E/E_0|$衰减的速度最快,以短波方向的透射峰波长 $\lambda_1 = 2\ 447.72$ nm为入射波长时内部局域电场最大值$|E/E_0|$衰减速度次之,而以长波方向的透射峰波长 $\lambda_3 = 2\ 675.13$ nm 为入射波长时内部局域电场最大值$|E/E_0|$的衰减速度最慢。进一步可以推测,当正虚部 k 值增大到一定数值时,光量子阱内部局域电场将趋于零,此时宏观上表现为分立透射峰的透射率为零,即光量子阱可实现光学全反射镜功能。

当 A 介质掺入增益效应的激活杂质,取 $\varepsilon_A = 6.670 - k$i 时,并取 $k = 0$、0.04、0.06...、0.12、0.16,仍分别以 $\lambda_1 = 2\ 447.72$ nm、$\lambda_2 = 2\ 556.21$ nm 和 $\lambda_3 = 2\ 675.13$nm 为入射波长,计算出的内部局域电场最大值对激活性杂质的响应曲线$|E/E_0| \sim |k|$,如图 8 所示。

从图 8 可见,当 A 介质中掺入具有增益效应的激活性杂质,即 A 介质的介电常数为含负虚部的复数时,光量子阱内部局域电场$|E/E_0|$最大值首先随负虚部$|k|$的增大而增大,当$|k|$增大到一定数值时,$|E/E_0|$最大值达到一个极大值,随后$|E/E_0|_{max}$随$|k|$的增大而下降,而且入射波长不同,内部局域电场最大值$|E/E_0|$极大值拐点不一样。以光量子阱短波方向的透射峰波长 $\lambda_1 = 2\ 447.72$ nm为入射波长,当$|k| = 0.10$ 时内部局域电场在$|E/E_0| = 299.60$ 最大值处出现拐点,以中心透射峰对应的波长 $\lambda_2 = 2\ 556.21$ nm 作为入射波长,当$|k| = 0.08$ 时内部局域电场在$|E/E_0| = 166.50$ 最大值处出现拐点,而以长波方向的透射峰波长 $\lambda_3 = 2\ 675.13$ nm 为入射波长,当$|k| = 0.10$时内部局域电场在$|E/E_0| = 52.196$ 最大值处出现拐点。可见,当介质 A 中掺入增益效应的激活杂质时,光量子阱的内部局域电场出现增益放大现象,而且增益放大的趋势相同,均为先增大后衰减,但不同波长的光量子阱内部局域电场增益放大极大值和对应的负虚部大小不同。

4 结 论

本文通过传输矩阵法研究光量子阱光传输特性对复介质的响应机制,得出如下结论:

(1)无论是实介质还是复介质,光量子阱内部局域电场均产生频率量子化并在透射谱中出现分立的窄透射峰。

(2)当掺入激活性杂质的复介质介电常数的虚部 k 为正值时,光量子阱内部局域电场和分立透射峰的透射率均出现衰减现象,而且正虚部 k 值越大,内部局域电场单调衰减越明显,但光量子阱不同波长位置的局域电场对正虚部 k 值的响应灵敏度不一样,其中光量子阱中心波长处对应的局域电场对正虚部 k 值响应最为灵敏。

(3)当掺入激活性杂质的复介质介电常数的虚部 k 为负值时,光量子阱内部局域电场和分立透射峰的透射率均出现增益放大现象,而且随着复介质介电常数的负虚部 $|k|$ 值增大,内部局域电场达到极大值后出现衰减现象,但不同波长位置的局域电场增益放大的极大值及其对应的负虚部 $|k|$ 大小不同,其中短波方向局域电场对负虚部 $|k|$ 值响应最灵敏度,长波方向局域电场对 $|k|$ 值响应灵敏度最低。

复介质对光量子阱光传输特性的调制机制,对新型光学滤波器、光学放大器和全反射镜的功能的研究和设计等,均具有积极的参考价值。

参考文献:

[1] YABLONOVITCH E. Inhibited spontaneous emission in solid-state physics and electronics[J]. *Physical Review Letters*, 1987, 58(20): 2059-2062.

[2] JOHN S. Strong localization of photons in certain disordered dielectric superlattices[J]. *Physical Review Letters*, 1987, 58(23): 2486-2489.

[3] 张峰, 张海鹍, 陈涛, 等. 掺钕双包层大模场保偏光子晶体光纤激光器[J]. 中国激光, 2017, 44(2): 0201020.
ZHANG F, ZHANG H K, CHEN T, *et al.*. Nd-doped double-clad large-mode-area polarization-maintaining photonic crystal fiber laser[J]. *Chinese Journal of Lasers*, 2017, 44(2): 0201020. (in Chinese)

[4] 陈颖, 曹会莹, 韩帅涛, 等. 含吸收介质的光子晶体法布里-珀罗异质结构的传感特性研究[J]. 光学学报, 2017, 37(2): 0223003. (in Chinese)
CHEN Y, CAO H Y, HAN SH T, *et al.*. Sensing property of photonic crystal fabry-pérot heterogeneous structure with absorption medium[J]. *Acta Optica Sinica*, 2017, 37(2): 0223003. (in Chinese)

[5] 李天琦, 毛小洁, 雷健, 等. 固体激光器与光纤激光器对光子晶体光纤棒耦合的分析与对比[J]. 中国光学, 2018, 11(6): 958-973.
LI T Q, MAO X J, LEI J, *et al.*. Analysis and comparison of solid-state lasers and fiber lasers on the coupling of rod-type photonic crystal fiber[J]. *Chinese Optics*, 2018, 11(6): 958-973. (in Chinese)

[6] 张琪,张红,周强,等.灭多威分子印迹光子晶体传感器的制备及应用[J].分析化学, 2019, 47(6): 883-889.
ZHANG Q, ZHANG H, ZHOU Q, *et al.*. Preparation and application of methomyl molecularly imprinted photonic crystal sensor [J]. *Chinese Journal of Analytical Chemistry*, 2019, 47(6): 883-889. (in Chinese)

[7] 王一飞,周丽君,杨吉,等.光子晶体纤维素膜检测二氧化硫气体[J].分析化学,2018, 46(9):1472-1478.
WANG Y F, ZHOU L J, YANG J, *et al.*. Detection of sulfur dioxide using cellulose photonic crystal membrane [J]. *Chinese Journal of Analytical Chemistry*, 2018, 46(9): 1472-1478. (in Chinese)

[8] 海一娜, 邹永刚, 田锟, 等. 水平腔面发射半导体激光器研究进展[J]. 中国光学, 2017, 10(2): 194-206.
HAI Y N, ZOU Y G, TIAN K, *et al.*. Research progress of horizontal cavity surface emitting semiconductor lasers[J].

Chinese Optics, 2017, 10(2): 194-206. (in Chinese)

[9] 刘继平, 李海波, 孟祥东, 等. 含点缺陷二维函数光子晶体的本征场分布[J]. 中国激光, 2018, 5(8): 0803001.
LIU J P, LI H B, MENG X D, *et al.*. Eigenfield distribution of two-dimensional functional photonic crystals with point defects[J]. *Chinese Journal of Lasers*, 2018, 45(8): 0803001. (in Chinese)

[10] 杜木青,张伶莉,刘永军.液晶及其不同填充结构对光子晶体光纤传输特性的影响[J].液晶与显示, 2018,33(2): 116-122.
DU M Q, ZHANG L L, LIU Y J. Effect of liquid crystal and its different filling structure on the transmission properties of photonic crystal fiber[J]. *Chinese Journal of Liquid Crystals and Displays*, 2018,33(2):116-122. (in Chinese)

[11] 马季, 吴向尧, 刘晓静, 等. 光子晶体缺陷层吸收特性的研究[J]. 中国激光, 2014, 41(3): 0306002.
MA J, WU X Y, LIU X J, *et al.*. Research on the absorption property of defect layer in photon crystals[J]. *Chinese Journal of Lasers*, 2014, 41(3): 0306002. (in Chinese)

[12] 孟宪芹,王维,谭纪风,等.光子晶体滤色实现五基色显示[J].液晶与显示, 2019,34(6): 576-581.
MENG X Q, WANG W, TAN J F, *et al.*. Application of photonic crystals for colorful display[J]. *Chinese Journal of Liquid Crystals and Displays*, 2019,34(6): 576-581. (in Chinese)

[13] 苏安, 王高峰, 蒙成举, 等. 光子晶体二元缺陷微腔的光传输特性[J]. 红外与激光工程, 2017, 46(6): 0620004.
SU A, WANG G F, MENG CH J, *et al.*. Light propagation characteristic of dual defect microcavity of photonic crystal [J]. *Infrared and Laser Engineering*, 2017, 46(6): 0620004. (in Chinese)

[14] 苏安, 蒙成举, 高英俊. 激活性杂质对光子晶体量子阱滤波器特性的调制[J]. 中国激光, 2014, 41(3): 0306001.
SU A, MENG CH J, GAO Y J. Modulation of activated impurity on filter property of photonic crystal quantum well[J]. *Chinese Journal of Lasers*, 2014, 41(3): 0306001. (in Chinese)

[15] 苏安, 蒙成举, 高英俊. 实现高品质滤波功能的一维光子晶体量子阱滤波器[J]. 中国激光, 2013, 40(10): 01006001.
SU A, MENG CH J, GAO Y J. Filter with one-dimensional photonic crystal quantum well possessing high-quality filtering functions[J]. *Chinese Journal of Lasers*, 2013, 40(10): 01006001. (in Chinese)

[16] 苏安, 高英俊. 双重势垒一维光子晶体量子阱的光传输特性研究[J]. 物理学报, 2012, 61(23): 234208.
SU A, GAO Y J. Light propagation characteristics of one-dimensional photonic crystal with double-barrier quantum well [J]. *Acta Physica Sinica*, 2012, 61(23): 234208. (in Chinese)

[17] 康永强, 高鹏, 刘红梅, 等. 单负材料组成一维光子晶体双量子阱结构的共振模[J]. 物理学报, 2015, 64(6): 064207.
KANG Y Q, GAO P, LIU H M, *et al.*. Resonant modes in photonic double quantum well structures with single-negative materials[J]. *Acta Physica Sinica*, 2015, 64(6): 064207. (in Chinese)

[18] 熊翠秀, 邓杨保, 邓曙光. 基于对称嵌套式光子晶体量子阱的多通道滤波器[J]. 激光与光电子学进展, 2016, 53(4): 041601.
XIONG C X, DENG Y B, DENG SH G. Multi-channel filter based on symmetric nested photonic crystals quantum well [J]. *Laser & Optoelectronics Progress*, 2016, 53(4): 041601. (in Chinese)

[19] 钟远聪. 光子晶体缺陷中掺入增益介质的小信号增益特性[J]. 人工晶体学报, 2014, 43(6): 1583-1587.
ZHONG Y C. Small signal gain characteristics of the defect photonic crystals with gain medium[J]. *Journal of Synthetic Crystals*, 2014, 43(6): 1583-1587. (in Chinese)

[20] 娄淑琴, 王智, 任国斌, 等. 具有复介电常量二维光子晶体的特性研究[J]. 光学学报, 2004, 24(3): 313-318.

LOU SH Q, WANG ZH, REN G B, *et al*.. The research on the properties of two-dimensional photonic crystal with the imaginary part of dielectric constant[J]. *Acta Optica Sinica*, 2004, 24(3): 313-318. (in Chinese)

作者简介：

Su An(1973—), male, born in Du'an, Guangxi. Professor, master degree. In 2009, he received his Master of Science degree from Guangxi University. Now he is working in the Department of Physics and Electronic Engineering, Hechi University, where he is mainly engaged in the research of photonic crystals. E-mail: suan3283395@163.com

苏　安(1973—)，男，广西都安人，教授，硕士学位，2009 年于广西大学获得理学硕士学位，现工作于河池学院 物理与机电工程学院，主要从事光子晶体方面的研究。E-mail: suan3283395@163.com

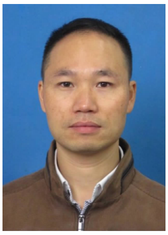

Meng Cheng-ju (1979—), male, born in Huaijiang, Guangxi. Senior Experimentalist, master degree. In 2016, he received his master degree from Guangxi University. Now he is working in the Department of Physics and Electronic Engineering, Hechi University, where he is mainly engaged in the research of photonic crystals. E-mail: mengchengju@163.com

蒙成举(1979—)，男，广西环江人，高级实验师，硕士学位，2016 年于广西大学获得工程硕士学位，现工作于河池学院物理与机电工程学院，主要从事光子晶体方面的研究。E-mail: mengchengju@163.com